Structural Transformations of Pb(II)−trans-1,2-bis(4′-pyridyl)ethene Coordination Polymers in Solution

ARTICLE *in* CRYSTAL GROWTH & DESIGN · SEPTEMBER 2011

Impact Factor: 4.89 · DOI: 10.1021/cg201071y

CRYSTAL GROWTH & DESIGN

ARTICLE

pubs.acs.org/crystal

Structural Transformations of Pb(II)-*trans*-1,2-bis(4′-pyridyl)ethene Coordination Polymers in Solution

Abdul Malik Puthan Peedikakkal and Jagadese J. Vittal*

Department of Chemistry, National University of Singapore, 3 Science Drive 3, Singapore 117543

Supporting Information

ABSTRACT:

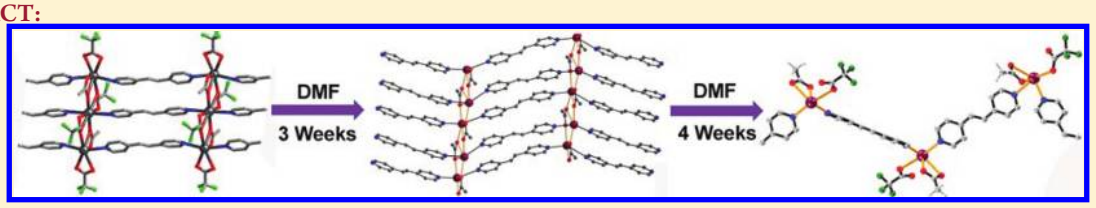

Reaction of bpe (bpe = *trans*-1,2-bis(4′-pyridyl)ethylene) with $Pb(OAc)_2 \cdot 3H_2O$ in the presence of trifluoroacetic acid (HTFA) affords a triple-stranded coordination polymer (CP) $[Pb_3(\mu\text{-bpe})_3(\mu\text{-}O_2CCF_3)_2(\mu\text{-}O_2CCH_3)_2(O_2CCF_3)_2]$ (**1**) in two days, which undergoes structural transformation in solution to yield a two-dimensional (2D) sheet-like CP $[Pb(\mu\text{-bpe})(\mu\text{-}O_2CCH_3)(O_2CCF_3)] \cdot 0.25bpe \cdot 1.75H_2O$ (**2**) in three weeks; finally compound **2** rearranges to $[Pb(\mu\text{-bpe})(O_2CCH_3)(O_2CCF_3)]$ (**3**) in the fourth week. Compound **3** has a molecular fabric-like interwoven structure formed by spiral one-dimensional (1D) coordination polymeric chains. Reaction of bpe with $Pb(O_2CCF_3)_2$ and $Pb(OAc)_2 \cdot 3H_2O$ respectively in equimolar ratio produces $[Pb(\mu\text{-bpe})(\mu\text{-}O_2CCF_3)_2]$ (**4**) and $[Pb(\mu\text{-bpe})(O_2CCH_3)_2] \cdot 0.25H_2O$ (**5**). The compound **4** is a three-dimensional (3D) CP with a $4^2.6^3.8$-**sra** ($SrAl_2$) topology, whereas **5** has a double-stranded structure with Pb(II)$\cdots\pi$ (pyridyl) interactions between 1D chains. The compounds $[Pb(\mu\text{-bpe})(\mu\text{-}O_2CCH_3)(O_2CCF_3)] \cdot 0.25bpe$ (**2a**), **4**, and **5** have been characterized by X-ray crystallography, while **1** and **3** were reported before. The factors influencing the rearrangement of CPs in solution have been discussed. The structural topological features observed in **2a**, **4**, and **5** have been attributed to the coordination preference of the Pb(II) and the carboxylate ligands.

INTRODUCTION

Despite its importance in photovoltaic conversion, organic light-emitting diodes, electroluminescence, and fluorescent sensors, less attention has been paid to the coordination polymers (CPs) of *p*-block metal ions.[1] Of these, lead(II) coordination polymeric frameworks inspired chemists because of the following reasons. Lead(II) has the ability to form diverse framework structures with interesting and rare topologies due to variable coordination geometries (2−10) with a large ionic radius.[2] It is the unique coordination preference and electronic intrinsic properties such as the presence of $6s^2$ lone pair on the outer electronic configuration that arouse immense interest in coordination chemistry, photophysics, and photochemistry.[3] Lead(II) CPs have been shown to have interesting photophysical properties such as luminescent[4] and birefringence.[5] It has the ability to form multidimensional Pb−X−Pb (X = O, N, Cl, S) inorganic−organic hybrid frameworks.[6]

It is well-known that the structural architectures of CPs can be varied by changing the metal−ligand ratio, solvents, geometry and size of the anions, pH and temperature, etc.[7] The flexibility of forming various topological structures can be enhanced by using *p*-block metals instead of transition metals. In the case of Pb(II), the coordination preference of the metal ion and its gometry, size, and bridging ability of the anions are expected to dictate the final topology of the CPs formed.[7c] On the other hand, dynamic solid-state structural transformations of CPs induced by light, heat, and small molecules have attracted immense interest and have been well studied.[8] However, only limited examples are available exhibiting structural transformation through a dissolution/recrystallization process.[9−11] The structural transformation in solution is expected to be mediated by solvents,[9a] acid/base or pH of the system,[9b] and ion exchange.[9c] The relative kinetic prevalence and thermodynamic stability also play important roles in slow dissolution of the parent crystals in solution and growth of the new crystalline phase. Rao, Natarajan, and co-workers reported several interesting transformations of low-dimensional zinc phosphates to complex open-framework structures on heating in water with or without added amines.[10] Lu and co-workers also encountered a number of dissolution/reorganization processes accompanying the structural rearrangement of three-dimensional (3D) CPs in aqueous lithium chloride or sodium chloride solutions.[11] Dynamic interconversion of compounds has also been observed in metallosupramollecular architectures formed from Pb(II) metal ions.[12] It is noted that the stereochemical activity of Pb(II) can be influenced by increasing the basicity of the ligands.[13]

While we are investigating the reaction of bpe (where bpe = 1,2-bis(4′-pyridyl)ethylene) with lead(II) acetate in the presence of trifluoroacetic acid (HTFA), we observed structural

Received: August 16, 2011
Published: September 16, 2011

Table 1. Crystallographic Data for 2a, 4, and 5

compounds	2a	4	5
formula	$C_{19}H_{15.5}F_3N_{2.5}O_4Pb$	$C_{32}H_{20}F_{12}N_4O_8Pb_2$	$C_{16}H_{16.5}N_2O_{4.25}Pb$
fw	607.03	1230.90	512.00
T/K	223(2)	293(2)	223(2)
cryst syst	orthorhombic	orthorhombic	monoclinic
space group	*Pbcn*	*Ccca*	*C2/c*
a/Å	19.509 (2)	20.530(7)	24.754(2)
b/Å	7.2877(4)	39.973(1)	9.862(8)
c/Å	28.124(1)	9.358(3)	13.407(1)
β/°	90	90	96.98(2)
vol/Å^3/Z	3998.7(4)/8	7680.1(4)/8	3248.8(5) /8
λ, Mg·cm^{-3}	2.017	2.129	2.094
μ/mm^{-1}	8.495	8.868	10.409
reflns col	26534	26009	11108
ind reflns/R_{int}/GOF	4593/0.0462/1.095	4416/0.0434/1.031	3732/0.0340/1.034
final $R[I > 2\sigma]$, R_1/wR_2	0.0370/0.0963	0.0245/0.0595	0.0241/0.0586

transformation of previously reported triple-stranded CP $[Pb_3(\mu\text{-bpe})_3(\mu\text{-}O_2CCF_3)_2(\mu\text{-}O_2CCH_3)_2(O_2CCF_3)_2]$ (**1**) to a two-dimensional (2D) sheet-like structure, $[Pb(\mu\text{-bpe})(\mu\text{-}O_2CCH_3)(O_2CCF_3)]\cdot 0.25bpe$ (**2a**) in solution through a dissolution/recrystallization process in three weeks. Compound **2** further rearranges to $[Pb(\mu\text{-bpe})(O_2CCH_3)(O_2CCF_3)]$ (**3**) in the fourth week. The structural transformation in solution is influenced by the presence of HTFA in dimethyl formamide (DMF) which appears to control the product formation and drives the more thermodynamically stable product. Further, the reaction of bpe with Pb(II)trifluoroacetate yields a 3D CP $[Pb(\mu\text{-bpe})(\mu\text{-}O_2CCF_3)_2]$ (**4**) having 2-fold interpenetrated net with **sra** topology. When bpe is reacted with lead(II) acetate alone produced one-dimensional (1D) CP, $[Pb(\mu\text{-bpe})(O_2CCH_3)_2]\cdot 0.25H_2O$ (**5**) having a double-stranded structure formed from Pb···π pyridyl interaction. A preliminary account of synthesis and structural features of **1** and **3** has already been appeared,[14,15] and we have also investigated the photoreactivity of **1** in the solid state.[14]

EXPERIMENTAL SECTION

Materials and Methods. All chemicals were purchased from commercial sources and used as received. All solvents used were of reagent grade. The synthetic procedures of $[Pb_3(\mu\text{-bpe})_3(\mu\text{-}O_2CCF_3)_2(\mu\text{-}O_2CCH_3)_2(O_2CCF_3)_2]$ (**1**) and $[Pb(\mu\text{-bpe})(O_2CCH_3)(O_2CCF_3)]$ (**3**) were reported previously.[14,15] The yields of **2**, **4**, and **5** were reported with respect to the metal salts. The ^{1}H NMR spectra were recorded in a Bruker ACF 300FT-NMR spectrometer with TMS as internal reference. Elemental analyses were performed in the Micro Analytical Laboratory, Department of Chemistry, National University of Singapore. Thermogravimetric analysis was carried out on a TA Instrument SDT 2960 TGA Thermal analyzer. Samples were heated at a constant rate of 5 °C min^{-1} from room temperature to 600 °C and at a continuous flow nitrogen atmosphere.

Synthetic Procedures. The syntheses of **2**−**5** are described below. However, the details of the reaction between bpe and lead(II) acetate in the presence of trifluoroacetic acid (HTFA) have been described in the Results and Discussion.

$[Pb(\mu\text{-bpe})(\mu\text{-}O_2CCH_3)(O_2CCF_3)]\cdot 0.25bpe\cdot 1.75H_2O$ (**2**). The colorless rod-like crystals[14] of **1** were left in the mother liquor (2 mL of DMF) in a beaker. A mixture of colorless cubic crystals of **2a** along with rod-like crystals of **1** was found after two weeks. The cubic crystals of **2** started to grow on the surface of disintegrated rod-like crystals of **1** in solution, and this process was completed in three weeks to get **2**. Yield: 0.056 g (18%). Elemental analysis (%) Calcd for $C_{19}H_{15.5}F_3N_{2.5}O_4Pb\cdot 1.75H_2O$ (607.03): C, 35.74; H, 2.99; N, 5.48. Found: C, 34.71; H, 1.97; N, 5.07. ^{1}H NMR (DMSO-d_6): δ_H 8.59 (d, 8H, δ-pyridyl proton), 7.61 (d, 8H, δ-pyridyl proton) 7.52 (s, 4H, −CH═CH−), 1.77 (s, 3H, CH_3-CO_2). Selected IR (KBr): ν (cm^{-1}) = 1687(s), 1630(s), 1598(s), 1502(m), 1409(s), 1188(s), 1133(s), 994(m), 965(s), 835(s), 812(m), 720(m), 667(m), 540(s). The single crystal **2a** used for structure determination does not have 1.75 water molecules as observed in the bulk.

$[Pb(\mu\text{-bpe})(\mu\text{-}O_2CCF_3)_2]$ (**4**). A mixture of $Pb(O_2CCF_3)_2$ (0.216 g, 0.5 mmol) and bpe (0.091 g, 0.5 mmol) in 6 mL of MeOH was stirred for 30 min. A white solid was precipitated out by the dropwise addition of diethyl ether into this mixture. The dried solid was dissolved in 6 mL of MeOH and taken in 12 fusion tubes. The experiment was conducted by diffusing 0.5 mL of the clear methanolic solution of the compound with 0.6 mL of diethyl ether. Colorless rod-like crystals were formed after 2 days. Yield: 0.26 g (84%). Elemental analysis (%) Calcd for $C_{16}H_{10}N_2F_6O_4Pb_1$ (615.46): C, 31.22; H, 1.64; N, 4.55; F, 18.52. Found: C, 31.21; H, 1.43; N, 4.65; F, 17.76. ^{1}H NMR (DMSO-d_6): δ_H 8.68 (d, 8H, δ-pyridyl proton), 7.76 (d, 8H, δ-pyridyl proton) 7.68 (s, 4H, −CH═CH−). Selected IR (KBr): ν (cm^{-1}) = 1686(s), 1598(s), 1501(w), 1427(s), 1205(s), 1133(s), 1071(m), 998(m), 971(m), 833(s), 804(m), 724(s), 545(s).

$[Pb(\mu\text{-bpe})(O_2CCH_3)_2]\cdot 0.25H_2O$ (**5**). A methanolic solution (0.2 mL) of bpe (0.018 g, 0.1 mmol) was layered over DMF/MeOH (0.5 mL/0.2 mL) solution of $Pb(OAc)_2\cdot 3H_2O$ (0.038 g, 0.1 mmol). Colorless block-like crystals were obtained after three days. Yield: 0.027 g (52%). Elemental analysis (%) Calcd for $C_{16}H_{16.5}N_2O_{4.25}Pb_1$ (512.01): C, 37.53; H, 3.25; N, 5.47. Found: C, 36.70; H, 3.08; N, 5.29. ^{1}H NMR (DMSO-d_6): δ_H 8.60 (d, 4H, δ-pyridyl proton), 7.60 (d, 4H, δ-pyridyl proton) 7.53 (s, 2H, −CH═CH−), 1.68 (s, 6H, CH_3-CO_2). Selected IR, (KBr, cm^{-1}) ν: 1625(m), 1600(s), 1559(s), 1410(s), 1343(m), 1205(m), 1070(m), 1001(s), 828(s), 721(s), 663(s), 546(s).

X-ray Crystallographic Analysis. Intensity data for **2a**, **4**, and **5** were collected on a Bruker APEX diffractometer attached with a CCD detector and graphite-monochromated Mo$K\alpha$ (λ = 0.71073 Å) radiation using a sealed tube (2.4 kW). Absorption corrections were made using the program SADABS,[16] and the crystallographic package SHELXTL[17] was used for all calculations. Crystal data as well as details of data collection and refinement of **2a**, **4**, and **5** are summarized in Table 1. In **2a**, the F atoms in $CF_3CO_2^-$ are disordered. Two sets of F

atoms were resolved forming hexagon when viewed along the C−C axis. The occupancy factors for the two models were refined to 0.65(1) and 0.35(1). The bpe situated along *b*-axis in the lattice was found to be disordered. Two models of bpe molecules slip-stacked along the *b*-axis have total occupancy of 0.25. Only U_{iso} was refined for the non-hydrogen atoms. The geometric parameters of the bpe molecule were fixed to ideal parameter using DFIX option. One of the CF_3 groups was found to be disordered in **4**. Two CF_3 groups were included in the model and their occupancy factors were refined to 0.58(2) and 0.42(2). Otherwise the anisotropic thermal parameter was refined for all non-hydrogen atoms. In **5**, the asymmetric unit contained 0.25 water. The positional parameters of these hydrogen atoms were refined but the U_{eq} was fixed at 0.08.

RESULTS AND DISCUSSION

Structural Transformation of Pb(II) CPs. When $Pb(OAc)_2 \cdot 3H_2O$ was reacted with bpe ligand in the presence of HTFA in a 1:1:1.3 molar ratio in DMF solution colorless long rod-like crystals of $[Pb_3(\mu\text{-bpe})_3(\mu\text{-}O_2CCF_3)_2(\mu\text{-}O_2CCH_3)_2(O_2CCF_3)_2]$ were produced after two days, which was reported by us before[14] (**1**). If the contents are left undisturbed, **1** slowly disintegrates in solution and undergoes structural transformation to give block-like cubic crystals of $[Pb(\mu\text{-bpe})(\mu\text{-}O_2CCH_3)(O_2CCF_3)] \cdot 0.25bpe \cdot 1.75H_2O$ (**2**) through a dissolution/recrystallization process (Figure S1, Supporting Information). The cubic crystals of **2** are formed along with rod-like crystals of **1** in two weeks, and after three weeks crystals of **2** are exclusively formed which were isolated and characterized by various techniques including X-ray crystallography. When the solution is left undisturbed, the crystals of $[Pb(\mu\text{-bpe})(O_2CCH_3)(O_2CCF_3)]$ (**3**) are isolated after a week as confirmed by X-ray powder diffraction (XRPD). As shown in Figure 1, the XRPD pattern for the product obtained after four weeks is exactly matched with that of **3**. An instant mixing of the components in a molar ratio of 1:1:1.3 has been used to produce pure **3** in bulk, while **1** has been obtained only by a slow evaporation method. It appears that **3** is a kinetic product, while **1** is a thermodynamic product. Such kinetic and thermodynamic products based on the rate of formation of precipitate have been observed by Kawano and Fujita et al.[18] During this reorganization process, the composition also changes, and thus three trifluoroacetate and one acetate ligand are lost for two [Pb(bpe)] fragments. However, 0.25 bpe ligand is retained inside the crystal lattice of **2**. After a period of time, cubic crystals of **2** are converted to block-like crystals of **3**. In this course, one bpe is removed and two-third of the DMF solution has been found to have evaporated along with the loss of TFA ligands. A change in the concentration of HTFA during slow evaporation of DMF in the mother liquor certainly influences the reorganization and product formation. Further, colorless rod-like crystals of $[Pb(\mu\text{-bpe})(\mu\text{-}O_2CCF_3)_2]$ (**4**) are obtained by the reaction of $Pb(O_2CCF_3)_2$ with bpe ligand in an equimolar ratio in MeOH. Similarly, when $Pb(OAc)_2 \cdot 3H_2O$ is reacted with bpe ligand in an equimolar ratio afforded $[Pb(\mu\text{-bpe})(O_2CCH_3)_2] \cdot (0.25H_2O)$ (**5**). On the other hand, colorless block-like crystals of zwitter-ionic coordination complex $[Pb(bpeH)_2(O_2CCF_3)_4]$ can be obtained by diffusion method from $Pb(O_2CCF_3)_2$, bpe, and HTFA in a molar ratio of 1:2:4 as noted by us before.[19] The bulk product of $[Pb(bpeH)_2(O_2CCF_3)_4]$ has been obtained in good yield by mixing bpe with $Pb(OAc)_2 \cdot 3H_2O$ and HTFA in methanol/CH_3CN (1:1 v/v) in an appropriate ratio, as confirmed by XRPD patterns (Figure S2, Supporting Information). However, this compound is formed comparatively in low yield even in the molar ratio of 1:1:3 or 1:1:1 because the protonation of pyridyl ring in bpe occurs rapidly with relatively higher HTFA acidity in methanol/CH_3CN.

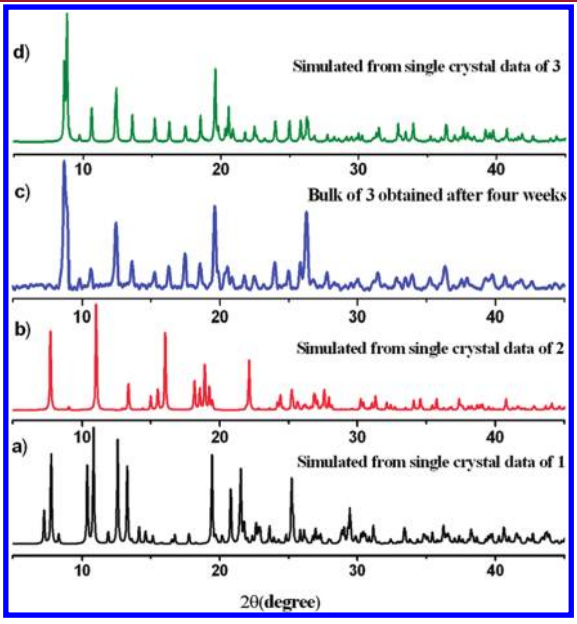

Figure 1. XRPD patterns of (a) simulated from the single crystal data of **1** (b) simulated from the crystal data of **2** (c) the bulk **3** obtained after four weeks (d) simulated from the crystal data of **3**.

Overall, the major changes occurring in the structures during the reorganization process can be summarized as shown in Scheme 1. The X-ray crystallographic structures of **2a**, **4**, and **5** are discussed in detail below.

Two-Dimensional Polymeric Structure of $[Pb(\mu\text{-bpe})(\mu\text{-}O_2CCH_3)(O_2CCF_3)] \cdot (0.25bpe)$ (2a). The 2D sheet comprises

Scheme 1. Structural Transformation of 1 to 2 in DMF Solution[a]

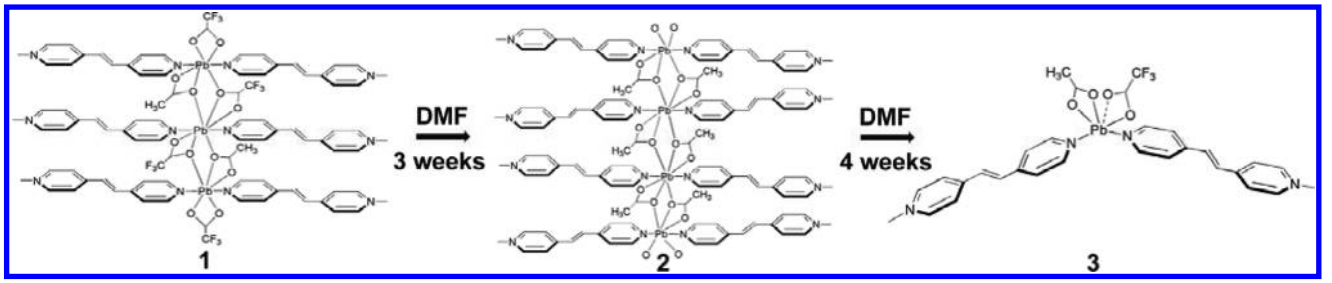

[a] Compound **2** finally transforms to **3** after a period of time.

dx.doi.org/10.1021/cg201071y |*Cryst. Growth Des.* 2011, 11, 4697–4703

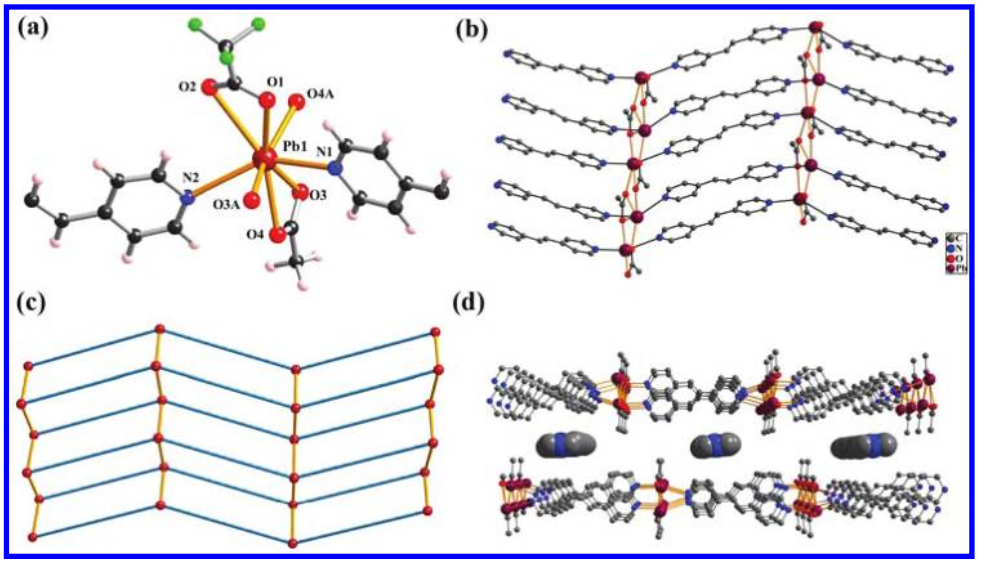

Figure 2. (a) Coordination geometry of Pb(II) metal center in **2a**. (b) A view of 2D sheet-like structure of **2a**. Trifluoroacetate and H-atoms are omitted for clarity. (c) A schematic representation of the 2D net is shown by connecting the Pb(II) metal centers. (d) Intercalation of bpe between the 2D layers in **2a**.

1D infinite chains of [Pb(μ-bpe)(O_2CCF_3)] bridged by acetate ligands. As shown in Figure 2a, the Pb(II) exhibits highly distorted eight-coordinate geometry by considering short-range atomic interactions. Six oxygen atoms are situated at the equatorial positions and two nitrogen atoms are at the epical positions in the PbO_6N_2 core (Figure 2a). Pb1 is unsymmetrically coordinated to the pyridyl nitrogen atoms of the bpe ligand occupying the axial positions [Pb(1)−N(1) 2.554(5) Å and Pb(1)−N(2)^f 2.896(6) Å (symmetry operator f: x, $1 - y$, $-1/2 + z$)]. The significant lengthening of Pb(1)−N(2)^f can be explained by the poor overlap of sp^3 lone pair of the nitrogen atom with the valence orbitals of Pb(II). Such longer Pb−N bond lengths are quite common in Pb(II) coordination compounds.[20] The $CF_3CO_2^-$ chelates to Pb1 through oxygen atoms in an asymmetric manner [Pb(1)−O(1) 2.616(5) Å and Pb(1)−O (2a) 2.95 Å]. The oxygen atoms of acetate ligand exhibit both bridging [Pb(1)−O(3A) 2.508(4) and Pb(1)−O(4A)^e 2.618(4) Å (symmetry operator e: $3/2 - x$, $1/2 + y$, z)] and chelating [Pb(1)−O(3)^e 2.674(4) and Pb(1)−O(4)^b 2.679(4) Å (symmetry operator b: x, $1 + y$, z)] modes. The Pb(μ-bpe) chains are propagating along the *c*-axis, while the acetate bridging along the *b*-axis led to the formation of corrugate 2D sheets in the *bc*-plane shown in Figure 2b and 2c. As a result, the bpe ligands are oriented parallel between the $Pb(OAc)_2$ array. However, the C═C double bonds between the adjacent bpe ligands in the 1D chain are oriented in a criss-cross fashion with a centroid C═C distance of 3.809 Å. Face-to-face $\pi\cdots\pi$ interaction between the pyridyl rings exists with an interplanar distance of 3.671(5) and 4.142(4) Å. Free bpe molecules are intercalated between the 2D layers inside the crystal lattice as shown in Figure 2d.

Three-Dimensional Polymeric Structure of [Pb(μ-bpe)(μ-O_2CCF_3)$_2$] (4). As shown in Figure 3a, metal center displays highly distorted six-coordinate geometry. Pb1 is strongly coordinated to the nitrogen atoms of the two bpe ligands [Pb(1)−N(1) 2.603(3) Å and Pb(1)−N(2) 2.445(3) Å], an oxygen atom of the $CF_3CO_2^-$ ligand [Pb(1)−O(1) 2.611(3) Å] and an oxygen of the neighboring monodentate $CF_3CO_2^-$ anion [Pb(1)−O(2A) 2.753(3) Å]. The metal center completes the geometry by chelating to $CF_3CO_2^-$ anion [Pb(1)−O(3) 2.405(3) Å and Pb(1)−O(4) 2.766(3) Å] in the position of acetate as seen in **3**.[15]

The basic repeating unit $[Pb(bpe)]^{2+}$ forms spiral 1D CP, and the packing of the polymer strands furnished the fabric-like structure similar to **3**.[15] However, the connectivity by the trifluoroacetate anions makes **4** different from **3**. The weak bonding found in **3** between the strands, that is, Pb1 and oxygen of the neighboring monodentate $CF_3CO_2^-$ anion [Pb1−O4 2.835(6) Å], becomes relatively strong [Pb1−O2 2.753(3) Å] in **4**. This $CF_3CO_2^-$ anion bridging between the polymeric strands makes **4** into a 3D CP. The crystallographic inversion center and glide plane present at the centers of the C═C bonds of the bpe ligand generate similar spiral 1D CPs as found in **3**.[15] The N1−Pb1−N2 angle 84.5(2)° is the same in both **3** and **4**. In **4**, the spiral chains are interlaced but interconnected through Pb1−O2 bonding between Pb1 and the oxygen atom of the neighboring monodentate $CF_3CO_2^-$ anion. As shown in Figure 4a, each strand crosses one over the next in almost parallel ABAB (where A strand = green and B strand = red) sequence as reported for **3**. A interlaced over B in **3**, however, B strand interconnected to A by μ_2(−O-C(CF_3)-O−) linkage, -AB-(−O-C(CF_3)-O)-AB- in **4** as shown in Figure 4b. Hence the interlacing causes interpenetration that results in **4** into a 3D net with doubly interpenetrated **sra** ($SrAl_2$) topology.[21]

Here the four Pb(II) octahedra are linked by two μ_2(−O-C(CF_3)-O−) and two μ_2-bpe bridges which form a square as shown in Figure 3b. Two N atoms at ∠N−Pb−N angle 84.5° and two O atoms of $Pb(O)_2$ linkages are situated at the vertex of tetrahedral node formed by Pb1. As a result, it forms an infinite zigzag ladder and Pb(II) atoms are situated at the vertices. Some of the reported frameworks, for example, MOF-69A,[21a] MOF-71[21b] and MIL-47,[21c] MIL-53[21d] have **sra** topologies and contain a similar zigzag ladder structure via carboxylate secondary building units (SBUs) units. Further these ladders are joined through bpe spacer links that result in **sra** topology as shown in Figure 3c. The Pb(II) atom represents the Al center which acts as tetrahedral node in **sra**. A single **sra** network in **4** contains a large void

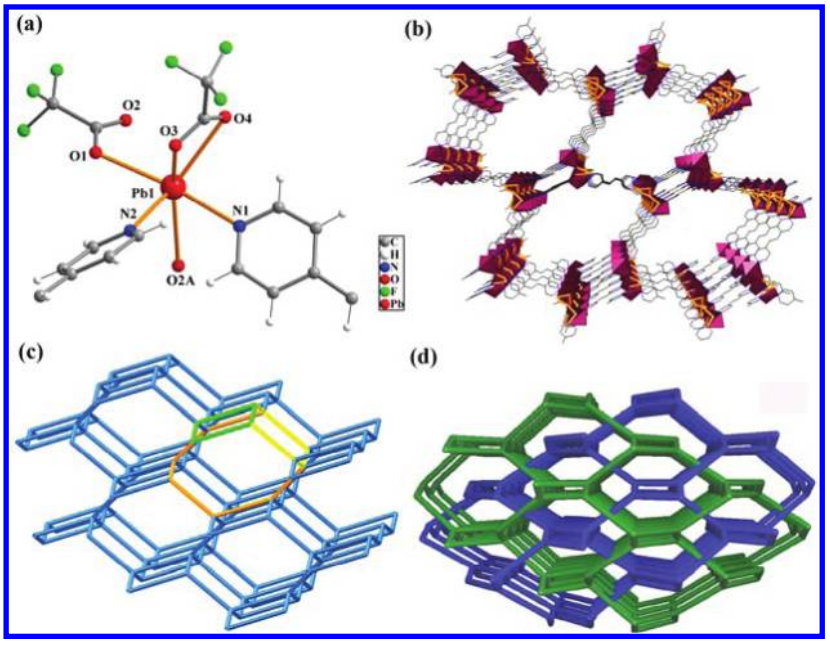

Figure 3. (a) A ball and stick diagram showing the asymmetric unit of **4**. Disordered F atoms are not shown. (b) A perspective view of 3D net formed by **4**. The octahedra Pb(II) atoms are indicated by polyhedra and yellow bonds indicate the (−O-C(CF_3)-O−) linkage. (c) A schematic representation of **sra** net formed by connecting Pb(II) nodes. Smallest circuits tetragon (green), hexagon (yellow), and octagon (orange) are shown in the net. (d) A perspective view of doubly interpenetrated **sra** nets in **4**.

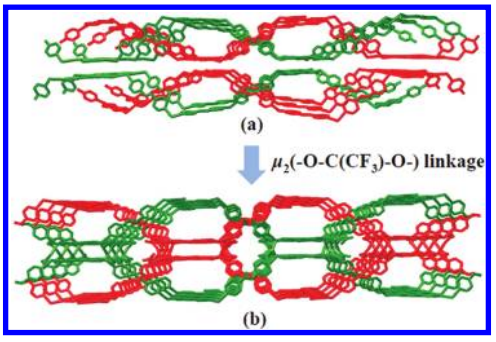

Figure 4. (a) Interlacing of 1D strands in **3** excluding weak interactions; (b) **sra** in **4** via μ_2(−O-C(CF_3)-O) linkage.

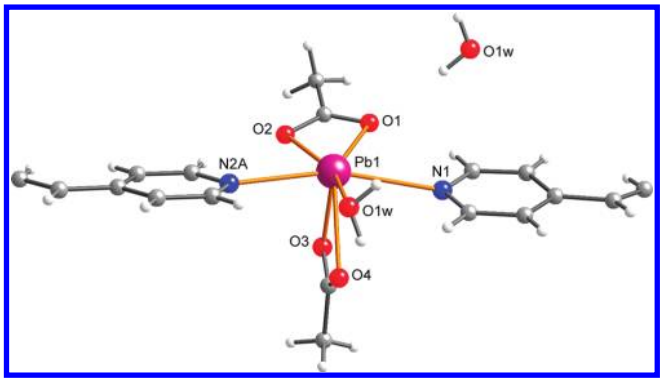

Figure 5. A perspective view of 5 showing the coordination enviornment at Pb1.

space having the size 31.29 Å × 18.05 Å. To eliminate the large void volume, it is occupied by another network, therefore doubly interpenetrated as shown in Figure 3d. As a result, **4** contains only 6.1%, total potential solvent area per unit cell.

Double-Stranded Coordination Polymeric Structure of [Pb(μ-bpe)(O_2CCH_3)$_2$]·0.25H_2O (5). As shown in Figure 5, the asymmetric unit of **5** contains the basic building block of the CP with 0.25 water molecule in the crystal lattice. The Pb1 displays a distorted octahedral geometry with PbO_4N_2 core and the Pb1 is coordinated to the nitrogen atoms of the bpe ligand [Pb(1)−N(1) 2.785(3) Å and Pb(1)−N(2) 2.684(3) Å] and chelates to two acetate ligands. There are three shorter [Pb(1)−O(1) 2.541(3); Pb(1)−O(2) 2.422(3); Pb(1)−O(3) 2.287(3) Å] and one relatively longer [Pb(1)−O(4) 2.773(3)] Pb−O bonds.

1D coordination polymeric chains are running approximately along the [101] direction. Interestingly, the adjacent 1D polymer pairs are interacting through Pb···π bonds between the Pb1 and the pyridyl rings of bpe ligands in η^6 mode as shown in Figure 6 to form double-stranded chains. The Pb1 interacts with nitrogen atom and five carbon atoms in the pyridyl ring. Although most of the distances fall below the sum of the van der Waals radii (Pb−N: 3.57 Å and Pb−C 3.72 Å), the Pb−C fall in the range of 3.8 Å but are still considered as weak Pb···C interaction.[22]

A survey of lead(II) structures containing Pb···π aryl interaction reveals that this interaction arises from the lead-bound lone-pair of electrons donated to the lowest unoccupied molecular orbital (LUMO) of the aryl ring. The survey was conducted by a CSD search using the following restrictions (Scheme 2): (i) the distance between the centroid of the aryl ring and the lead center (d) be equal to or less than 4.0 Å, and (ii) the angle, α defined by the vector perpendicular to the aryl ring (**V1**) and the vector passing through the centroid to the lead atom (**V2**), be equal or less than 20°.[22]

The average distance *d* is 3.46 Å found in reported Pb(II) compounds and the *d* range from a short 2.78 Å to a long 3.83 Å.[22]

dx.doi.org/10.1021/cg201071y |*Cryst. Growth Des.* 2011, 11, 4697–4703

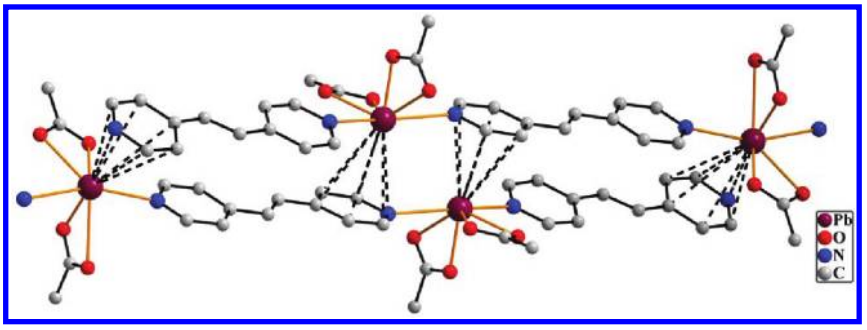

Figure 6. A portion of the 1D double-stranded CP **5** showing Pb···π pyridyl interactions. The Pb···π pyridyl distances range are 3.388(3)−3.737(4) Å.

Scheme 2. Representation of Geometric Parameters Defining the Intermolecular Pb···π Interactions[22]

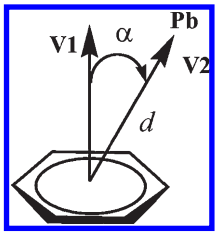

There is only one example found in which a ladder is formed by linking two polymeric strands via Pb···π aryl contacts.[23] Although Pb···π aryl interaction is known but it is rarely observed. A similar CSD search[24] using the above criteria on Pb···π pyridyl interaction furnished three hits containing potential Pb···π pyridyl interaction involving phenanthroline[25] and naphthalene rings.[26] The third example is the intramolecular Pb···π pyridyl interaction in a coordination complex.[27] However, Pb···π pyridyl interaction remains unknown in CPs.

The perpendicular distance (d) between the centroid of the pyridyl ring in Scheme 2 and the Pb(II) center in **5** is equal to 3.26 Å (i.e., < 4 Å) and the angle α is 20°. Here considerable intermolecular Pb···π pyridyl interaction is expected due to the lone-pair of electrons donation to the LUMO of the pyridyl ring supported by the bond angles observed around the metal geometry and bond angle between the pyridyl ring and Pb(II) metal center. The spacial distribution of the ligands around the highly distorted metal geometry indicates an identifiable void (or gap) in the distribution of bonds to the ligands represent the active lone pair at Pb(II) metal center. The lone pair is mostly situated in the *trans* position to the very short Pb(1)−O(3) bond. The lone-pair/bond-pair repulsion results in a comparatively long Pb(1)−O(4) bond. The bond angles distortion in O(1)−Pb(1)−O(4) 133.70(11)°, O(2)−Pb(1)−O(4) 129.20(9)°, N(1)−Pb(1)−N(2)^a 160.5(1)° (symmetry operator a = $x - 1/2, y + 1/2, z + 1/2$) around the metal geometry also supports the presence of an active lone pair. Lone-pair···π interaction is considered as one of the supramolecular synthon in crystal engineering[28] and is current interest due to the stabilized lone-pair···π intermolecular interactions in protein structures.[29] The Pb···π pyridyl interaction acts as a supramolecular synthon to furnish zero-dimensional aggregates, 1D linear chains, 2D arrays, and 3D networks.[23] Here in **5**, the Pb···π pyridyl interaction results in the aggregation of 1D CPs to a double-stranded structure.

1D to 3D CPs. The properties of Pb(II) metal ions and ligands certainly control the formation of different topological structures. A close examination of the metal centers and organic connectivities indicates that the ∠N−Pb−N bite angle variation and Pb−O−Pb linkages influence the formation of dimensionality of CPs in **1**−**5**. It is widely known that the *trans* ∠N−M−N bite angle can influence the conformation of 1D CPs (linear or zigzag).[30,31] The ∠N−Pb−N bite angle in this study significantly varies from 83.4(2)° to 180° and contributes to the formation of different topological structures. A considerable decrease is observed from 160.5° (**5**) to 83.4° (**3**) when half of the acetate is replaced by trifluoroacetate ligands. However, this angle is retained in **4** (84.5°) and $[Pb(bpeH)_2(O_2CCF_3)_4]$[19] (84.5°) by replacing all the acetate by trifluoroacetate ligands. The zigzag spiral conformation in **3**, **4**, and $[Pb(bpeH)_2(O_2CCF_3)_4]$[19] is due to this decrease in the bite angle. There are two ∠N−Pb−N angles observed in triple-stranded ladder (**1**); N1−Pb1−N2 180° and N3−Pb2−N3A 160°. This angle is decreased in **2a** (144.1°) which results in a weak Pb1−N2 bond. The *holodirected*[30] hexagonal-bipyramidal metal geometry found Pb2 in **1**. However the distortion is reflected in the bite angles from 180° Pb1 in **1**, **2a** and **5**, around the *hemidirected*[30] metal geometries.

The monocarboxylates involve in chelating and bridging modes and from monodentate (**3**) to tridentate (**1**) bonding modes. However, the $CF_3CO_2^-$anion in **2a** chelates but is not involved in bridging. A discrete $Pb_3(O)_8$ connectivity (rungs of the ladder) in **1** resulted from two acetates and two trifluoroacetate using via $\mu_{1,3}$ mode. An infinite $Pb(O)_2$ connectivity ($\mu_{1,3}$ mode) results in 2D CP in **2a**. The two O atoms of $Pb(O)_2$ connectivity are situated at the vertex of the tetrahedral node formed by the Pb(II) metal center in **4**, and this results in the 3D network of **sra** topology.

CONCLUSIONS

Reactivity of Pb(II) metal ion with bpe has been investigated in the presence of acetate and trifluoroacetate anions. A triple-stranded 1D CP (**1**) undergoes structural transformation in solution to produce a 2D sheet-like CP (**2a**) which rearranges to a zigzag 1D CP (**3**). The compound **3** exhibits a molecular fabric structure. Interestingly, the structure of compound **4** containing the trifluoroacetate anion closely resembles that of **3**. However, infinite Pb−O(CCF3)−O−Pb linkage in **4** results in a doubly interpenetrated 3D network with **sra** topology. On the other hand, the reaction of Pb(II) acetate with bpe in a 1:1 ratio affords linear 1D CP, but the Pb···π pyridyl interactions generate a double-stranded (or ladder-like) structure. The

topological variation of the structures has been attributed to the coordination preference of the Pb(II) metal ion and bridging ability of anionic carboxylate ligands. In all the compounds, the metal geometry is heavily distorted *hemidirected* except the Pb2 metal center in **1** which is expected due to the influence of hard oxygen donor carboxylate ligands.

■ ASSOCIATED CONTENT

Supporting Information. Crystallographic information files (CIF) and bond length and angles for **2a**, **4**, and **5**. Thermal analysis of **1**−**5**. This material is available free of charge via the Internet at http://pubs.acs.org

■ AUTHOR INFORMATION

Corresponding Author

*Tel: +65 6516 2975. Fax: +65 6779 1691. E-mail: chmjjv@nus.edu.sg.

■ ACKNOWLEDGMENT

We thank Ministry of Education for funding this project through NUS FRC Grant No. R-143-000-439-112 and Ms. Geok Kheng Tan and Ms. Hong Yimian for the collection of X-ray crystallographic data.

■ REFERENCES

(1) (a) Vogler, A.; Nikol, H. *Pure Appl. Chem.* **1992**, *64*, 1311–1317. (b) Strasser, A.; Vogler, A. *J. Photochem. Photobiol. A* **2004**, *165*, 115–118.

(2) (a) Yang, J.; Ma, J. F.; Liu, Y. Y.; Ma, J. C.; Batten, S. R. *Inorg. Chem.* **2007**, *46*, 6542–6555. (b) Fan, S. R.; Zhu, L. G. *Inorg. Chem.* **2007**, *46*, 6785–6793. (c) Zhao, Y. H.; Xu, H. B.; Fu, Y. M.; Shao, K. Z.; Yang, S. Y.; Su, Z. M.; Hao, X. R.; Zhu, D. X.; Wang, E. B. *Cryst. Growth Des.* **2008**, *8*, 3566–3576. (d) Yang, J.; Ma, J. F.; Liu, Y. Y.; Ma, J. C.; Batten, S. R. *Cryst. Growth Des.* **2009**, *9*, 1894–1911. (e) Yang, J.; Li, G. D.; Cao, J. J.; Yue, Q.; Li, G. H.; Chen, J. S. *Chem.—Eur. J.* **2007**, *13*, 3248–3261.

(3) (a) Deo, S. H.; Godwin, A. *J. Am. Chem. Soc.* **2000**, *122*, 174–175. (b) Li, J.; Lu, Y. *J. Am. Chem. Soc.* **2000**, *122*, 10466–10467. (c) Jack, M. H.; Saeed, M.; Ali, A. S. *Inorg. Chem.* **2004**, *43*, 1810–1812. (d) Li, L. K.; Song, Y. L.; Hou, H. W.; Fan, Y. T.; Zhu, Y. *Eur. J. Inorg. Chem.* **2005**, 3238–3249.

(4) (a) Zhao, Y.-H.; Xu, H.-B.; Fu, Y.-M.; Shao, K.-Z.; Yang, S.-Y.; Su, Z.-M.; Hao, X.-R.; Zhu, D.-X.; Wang, E.-B. *Cryst. Growth Des.* **2008**, *8*, 3566–3576. (b) Zhao, Y.-H.; Xu, H.-B.; Shao, K.-Z.; Xing, Y.; Su, Z.-M.; Ma, J.-F. *Cryst. Growth Des.* **2007**, *7*, 513–520. (c) Zhang, K.-L.; Zhou, F.; Wu, R.; Yang, B.; Ng, S. W. *Inorg. Chim. Acta* **2009**, *362*, 4255–4259.

(5) (a) Katz, M. J.; Kaluarachi, H.; Batchelor, R. J.; Bokov, A. A.; Ye, Z.-G.; Leznoff, D. B. *Angew. Chem., Int. Ed.* **2007**, *46*, 8804–8807. (b) Katz, M. J.; Aguiar, P. M.; Batchelor, R. J.; Bokov, A. A.; Ye, Z.-G.; Kroeker, S.; Leznoff, D. B. *J. Am. Chem. Soc.* **2006**, *128*, 3669–3676.

(6) (a) Rao, K. P.; Thirumurugan, A.; Rao, C. N. R. *Chem.—Eur. J.* **2007**, *13*, 3193–3201. (b) Thirumurugan, A.; Sanguramath, R. A.; Rao, C. N. R. *Inorg. Chem.* **2008**, *47*, 823–831.

(7) (a) Batten, S. R.; Neville, S. M.; Turner, D. R. *Coordination Polymers: Design, Analysis and Applications*; RSC Publishing: Cambridge, 2009. (b) Leong, W. L.; Vittal, J. J. *Chem. Rev.* **2011**, *111*, 688–764. (c) Diaz, P.; Benet-Buchholz, J.; Vilar, R.; White, A. J. P. *Inorg. Chem.* **2006**, *45*, 1617–1626.

(8) (a) Kitagawa, S.; Kitaura, R.; Noro, S.-i. *Angew. Chem., Int. Ed.* **2004**, *43*, 2334 and references therein. (b) Kitagawa, S.; Uemura, K. *Chem. Soc. Rev.* **2005**, *34*, 109 and references therein. (c) Vittal, J. J. *Coord. Chem. Rev.* **2007**, *251*, 1781 and references therein.

(9) (a) Wu, H. C.; Thanasekaran, P.; Tsai, C. H.; Wu, J. Y.; Huang, S. M.; Wen, Y. S.; Lu, K. L. *Inorg. Chem.* **2006**, *45*, 295–303. (b) Karabach, Y. Y.; Kirillov, A. M.; da Silva, M. F. C. G.; Kopylovich, M. N.; Pombeiro, A. J. L. *Cryst. Growth Des.* **2006**, *6*, 2200–2203. (c) Zhang, J.-J.; Zhao, Y.; Gamboa, S. A.; Lachgar, A. *Cryst. Growth Des.* **2008**, *8*, 172–175. (d) Kim, H.-J.; Lee, J.-H.; Lee, M. *Angew. Chem., Int. Ed.* **2005**, *44*, 5810–5814. (e) Lidrissi, C.; Romerosa, A.; Saoud, M.; Serrano-Ruiz, M.; Gonsalvi, L.; Peruzzini, M. *Angew. Chem., Int. Ed.* **2005**, *44*, 2568–2572. (f) Murugavel, R.; Sathiyendiran, M.; Pothiraja, R.; Walawalkar, M. G.; Mallah, T.; Rivière, E. *Inorg. Chem.* **2004**, *43*, 945–953.

(10) (a) Dan, M.; Rao, C. N. R. *Chem. Commun.* **2003**, 2212–2213. (b) Natarajan, S.; Rao, C. N. R. *J. Mater. Chem.* **2001**, *11*, 1537–1546. (c) Ayi, A. A.; Choudhury, A.; Natarajan, S.; Neeraj, S.; Rao, C. N. R. *J. Mater. Chem.* **2001**, *11*, 1181–1191. (d) Padmanabhan, M.; Joseph, J. C.; Thirumurugan, A.; Rao, C. N. R. *Dalton Trans.* **2008**, 2809–2811.

(11) (a) Ding, M.-T.; Wu, J.-Y.; Liu, Y.-H.; Lu, K.-L. *Inorg. Chem.* **2009**, *45*, 295–303. (b) Wu, J.-Y.; Yang, S.-L.; Luo, T.-T.; Liu, Y.-H.; Cheng, Y.-W.; Chen, Y.-F.; Wen, Y.-S.; Lin, L.-G.; Lu, K.-L. *Chem.—Eur. J.* **2008**, *14*, 7136–7139. (c) Wu, J.-Y.; Ding, M.-T.; Wen, Y.-S.; Liu, Y.-H.; Lu, K.-L. *Chem.—Eur. J.* **2009**, *15*, 3604–3614.

(12) Barboiu, M.; Vaughan, G.; Graff, R.; Lehn, J.-M. *J. Am. Chem. Soc.* **2003**, *125*, 10257–65.

(13) Katz, M. J.; Michaelis, V. K.; Aguiar, P. M.; Yson, R.; Lu, H.; Kaluarachchi, H.; Batchelor, R. J.; Schreckenbach, G.; Kroeker, S.; Patterson, H. H.; Leznoff, D. B. *Inorg. Chem.* **2008**, *47*, 6353–6363.

(14) Peedikakkal, A. M. P.; Vittal, J. J. *Inorg. Chem.* **2010**, *49*, 10–12.

(15) Peedikakkal, A. M. P.; Vittal, J. J. *Cryst. Growth Des.* **2008**, *8*, 375–377.

(16) Sheldrick, M. *SADABS*, version 2.05; University of Göttingen: Göttingen, Germany.

(17) Sheldrick, G. M. *SHELXS-97, Program for X-ray Crystal Structure Solution*; University of Göttingen: Germany, 1997.

(18) Kawano, M.; Haneda, T.; Hashizume, D.; Izumi, F.; Fujita, M. *Angew. Chem., Int. Ed.* **2008**, *47*, 1269–1271.

(19) Peedikakkal, A. M. P.; Koh, L. L.; Vittal, J. J. *Chem. Commun.* **2008**, 441–443.

(20) (a) Fleischer, H.; Schollmeyer, D. *Inorg. Chem.* **2004**, *43*, 5529–5536. (b) Bondi, A. *J. Phys. Chem.* **1964**, *68*, 441–452.

(21) (a) Rosi, N. L.; Eddaoudi, M.; Kim, J.; O'Keeffe, M.; Yaghi, O. M. *Angew. Chem., Int. Ed.* **2002**, *41*, 284–287. (b) Rosi, N. L.; Kim, J.; Eddaoudi, M.; Chen, B. L.; O'Keeffe, M.; Yaghi, O. M. *J. Am. Chem. Soc.* **2005**, *127*, 1504–1518. (c) Barthelet, K.; Marrot, J.; Riou, D.; Férey, G. *Angew. Chem., Int. Ed.* **2002**, *41*, 281–284. (d) Serre, C.; Millange, F.; Thouvenot, C.; Noguès, M.; Marsolier, G.; Louër, D.; Férey, G. *J. Am. Chem. Soc.* **2002**, *124*, 13519.

(22) Tiekink, E. R. T.; Zukerman-Schpector, J. *Aust. J. Chem.* **2010**, *63*, 535–543.

(23) Yang, J.; Li, G.-D.; Cao, J.-J.; Yue, Q.; Li, G.-H.; Chen, J.-S. *Chem.—Eur. J.* **2007**, *13*, 3248–3261.

(24) CSD search: October 2009 using CONQUEST version 1.11

(25) Du, Z.-Y.; Xu, H.-B.; Li, X.-L.; Mao, J.-G. *Eur. J. Inorg. Chem.* **2007**, 4520–4529.

(26) Wang, W. *Chin. J. Inorg. Chem.* **2007**, *23*, 1040–1044.

(27) Leung, W.-P.; Wong, K.-W.; Wang, Z.-X.; Mak, T. C. W. *Organometallics* **2006**, *25*, 2037–2044.

(28) (a) Mooibroek, T. J.; Gamez, P.; Reedijk, J. *CrystEngComm* **2008**, *10*, 1501–1510. (b) Tiekink, E. R. T.; Zukerman-Schpector, J. *CrystEngComm* **2009**, *11*, 1176–1186.

(29) (a) Egli, M.; Sarkhel, S. *Acc. Chem. Res.* **2007**, *40*, 197–205. (b) Sarkhel, S.; Rich, A.; Egli, M. *J. Am. Chem. Soc.* **2003**, *125*, 8998–8999.

(30) Shimoni-Livny, L.; Glusker, J. P.; Bock, C. W. *Inorg. Chem.* **1998**, *37*, 1853–1867.

(31) Ye, B.-H.; Tong, M.-L.; Chen., X.-M. *Coord. Chem. Rev.* **2005**, *249*, 545–567.